ELSEVIER

Contents lists available at ScienceDirect

# Ecotoxicology and Environmental Safety

journal homepage: www.elsevier.com/locate/ecoenv





# Perfluorooctane sulfonate (PFOS), a novel environmental pollutant, induces liver injury in mice by activating hepatocyte ferroptosis

Yang Yang <sup>a,1</sup>, Liuwei Xie <sup>b</sup>, Yu Zhu <sup>c,1</sup>, Yongjia Sheng <sup>c</sup>, Jin Wang <sup>c</sup>, Xiaohong Zhou <sup>c</sup>, Wenyan Li <sup>c</sup>, Chenxi Cao <sup>c,\*</sup>, Yi Yang <sup>c,\*</sup>, Chenyang Han <sup>d,\*</sup>

- <sup>a</sup> Shenyang Medical College, China
- b Criminal Investigation Police University of China, China
- <sup>c</sup> The Second Affiliated Hospital of Jiaxing University, China
- <sup>d</sup> Department of pharmacy, The Second Affiliated Hospital of Jiaxing University, 314001, China

#### ARTICLE INFO

Edited by Professor Bing Yan

Keywords:
PFOS
Liver injury
Ferroptosis
Toxicology
Environmental toxin

#### ABSTRACT

*Objective*: We investigated the toxicological mechanism by which perfluorooctane sulfonate (PFOS) induces liver injury via ferroptosis.

Methods: Primary mouse hepatocytes were treated with LD50 = 55 M PFOS. Their cytotoxicity was detected by CCK-8 and LDH assays, while JC-1 staining was used to identify their mitochondrial membrane potential. GSH-Px, MDA, and SOD levels were determined using kits, and Fe2 + levels were determined using the FerroOrange probe and iron ion assay kit. The DCFH-DA probe was used to examine ROS levels, while Western blot was used to examine protein expressions. After treatment with the ferroptosis inhibitor YL939 and the ROS inhibitor BABTA, the ability of PFOS to induce ferroptosis was observed. In animal experiments, we examined the liver function and the degree of hepatic ferroptosis of mice treated with PFOS as well as their histopathological changes.

Results: PFOS could induce hepatocyte ferroptosis, while YL939 and BABTA treatment could inhibit PFOS-induced ferroptosis. PFOS could induce liver injury and increase ferroptosis levels in tissue, while treatment with YL939 and BABTA could inhibit liver injury.

Conclusion: PFOS can induce ferroptosis in hepatocytes and cause liver injury in mice, which is its toxicological mechanism.

# 1. Background

As a common surfactant and plasticizer, perfluorooctane sulfonate (PFSO) is often used in industry, which has also led to significant environmental pollution in recent years (Phelps et al., 2023). Due to its extreme persistence, PFSO is the most difficult to degrade organic pollutant that can remain in the environment for a long time (Zhang et al., 2023). Meanwhile, PFOS can accumulate in organic organisms. Numerous evidences have shown that the organisms of the aquatic food chain have a strong PFOS accumulating effect (Rudzanova et al., 2023). Through the accumulation effect of aquatic organisms and the food chain, PFOS in water is transferred to higher organisms that include humans (Liu et al., 2023a). Currently, high levels of PFOS have been discovered in higher animals (Zhao et al., 2023). Studies on the toxicity

of PFOS have found that PFOS is hepatotoxic, affects lipid metabolism, reduces the sperm count of experimental animals, and increases the number of abnormal sperm (Mohona et al., 2023). PFOS leads to an increase in peroxide production in several body organs, which leads to oxidative damage and directly or indirectly damages the genetic material, thereby triggering tumors (Wang et al., 2023; Wu et al., 2023). Nevertheless, the specific mechanism of PFOS-induced liver injury is not yet fully understood.

Ferroptosis, which mainly catalyzes the highly expressed unsaturated fatty acids on the cell membranes and leads to lipid peroxidation through the action of divalent iron or ester oxygenase, thus inducing apoptosis (Qian et al., 2023). In addition, it is also manifested by a decrease in GPX4, the core regulatory enzyme of the antioxidant system (glutathione). Activation of the oxidative stress system is a major

E-mail addresses: caochenxi-jxey@hotmail.com (C. Cao), wasd911@126.com (Y. Yang), 691513770@qq.com (C. Han).

<sup>\*</sup> Corresponding authors.

<sup>&</sup>lt;sup>1</sup> Co-First author: Yang Yang and Yu Zhu

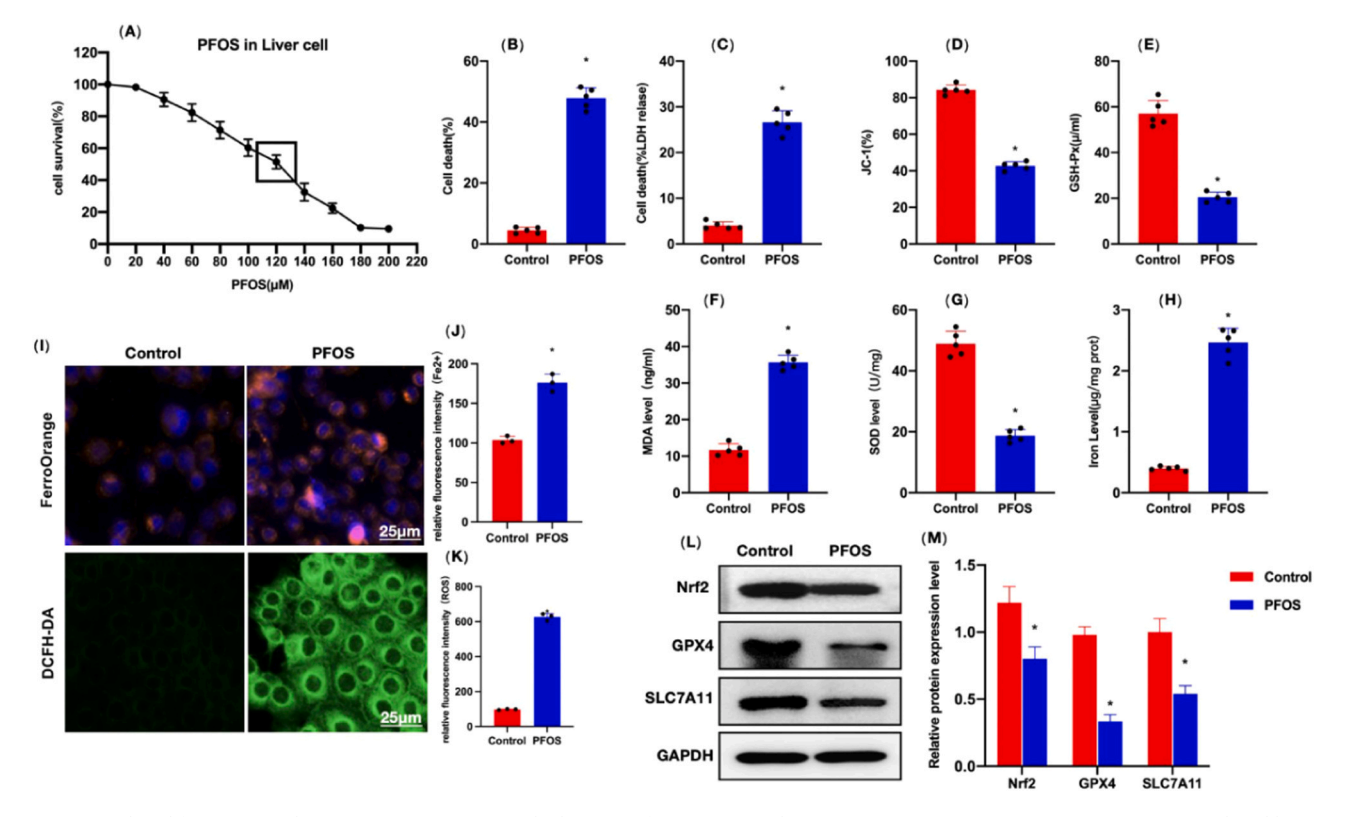


Fig. 1. : PFOS induced ferroptosis in hepatocytes. A: LD50, PFOS had a LD50 of 55 μM against hepatocyte injury B-C: Cytotoxicity (n = 5), PFOS induced hepatocyte injury and elevated the levels of cell damage and LDH D: JC-1 (n = 5), mitochondrial damage and significantly reduced proportion of JC-1 were noted in the PFOS group E-G: GSH-Px, MDA and SOD (n = 5), PFOS could downregulate the GSH-Px and SOD levels, while elevating the MDA level H: Iron ion (n = 5), PFOS could elevate the intracellular Fe<sup>2+</sup> levels I-K: IF (n = 5), the Fe<sup>2+</sup> and ROS levels were obviously upregulated in the PFOS group, where the fluorescence intensity was shown to be higher than that in the Control group L-M: Relative protein expressions (n = 5), PFOS could inhibit the levels of Nrf2, GPX4 and SLC7A11. \*P < 0.05 vs. Control.

mechanism of ferroptosis, and ROS and GPX4 play crucial roles in ferroptosis (Liu et al., 2023b; Li et al., 2023a). This study provides a new mechanism of PFOS-induced hepatotoxicity by combining ferroptosis with the liver toxicology of PFOS.

#### 2. Materials and methods

# 2.1. Cell model

We used PFOS gradient concentrations to treat primary mouse hepatocytes (Procell Biotechnology, Wuhan, China) for 24 h. Primary mouse hepatocytes are cultured in a special culture medium (Procell Biotechnology, Wuhan, China). The LD50 of PFOS was determined by CCK-8 assay and revealed that LD50 = 55 M. In the cell experiments, we set the concentration of PFOS to 55 M and the treatment time to one day. In mechanism research, 6 h preprocessing was performed with ferroptosis inhibitor YL939 (0.25 M) and ROS inhibitor BABTA (1.0 M), respectively, to inhibit the activation of ferroptosis and ROS.

#### 2.2. CCK-8

Hepatocytes were treated with PFOS for 24 h and then their cytotoxicity was detected by CCK-8 assay. After adding 100 L of phenol redfree medium and 10 L of CCK-8 reagent (MCE, Shanghai, China) to each well of 96-well microtiter plates, hepatocytes were incubated in a threegas incubator for 4 h. OD values were measured at 450 nm after medium replacement and cytotoxicity was calculated. Results were expressed as  $\%\pm SE$ .

#### 2.3. LDH

Lactate dehydrogenase assay was used to detect the cytotoxicity of PFOS. After intervening hepatocytes with PFOS for 24 h, the LDH release rate was measured following the instructions of LDH kit (Solarbio, Beijing, China), and the results were shown as  $\%\pm$  SE.

#### 2.4. JC-1

Mitochondria in tissues and cells have been detected. Mouse liver tissues were cut into pieces, placed in PMSF solution at a ratio of 1:10, and centrifuged at 1000 g for 5 min. The resulting sediment consisted of mitochondria, which were diluted and added to the 96-well microtiter plate for JC-1 staining (Beyotime Biotechnology, Shanghai, China). The JC-1 working solution was added to the mitochondrial solution at a ratio of 1:10 for a 30-minute incubation time of 10  $\mu g/mL$ . The JC monomers were identified at 490/530 nm, while the JC-1 polymers were identified at 525/590 nm. The polymer/monomer ratio was statistically analyzed. Intracellular JC-1 detection was performed by flow cytometry and the results were expressed as  $\% \pm$  SE.

#### 2.5. Iron ion (Fe2 +) assay

The tissues/cells were homogenized with PBS, centrifuged at 2500 g, and then the supernatant was collected and bathed in boiling water for 5 min using double distilled water, 2 mg/L standard iron solution and chromogenic reagent according to the instructions of iron ion assay kit (Jiancheng Bioengineering Institute, Nanjing, China). After cooling and centrifugation at 3500 g, the OD value of supernatant was measured at 520 nm.

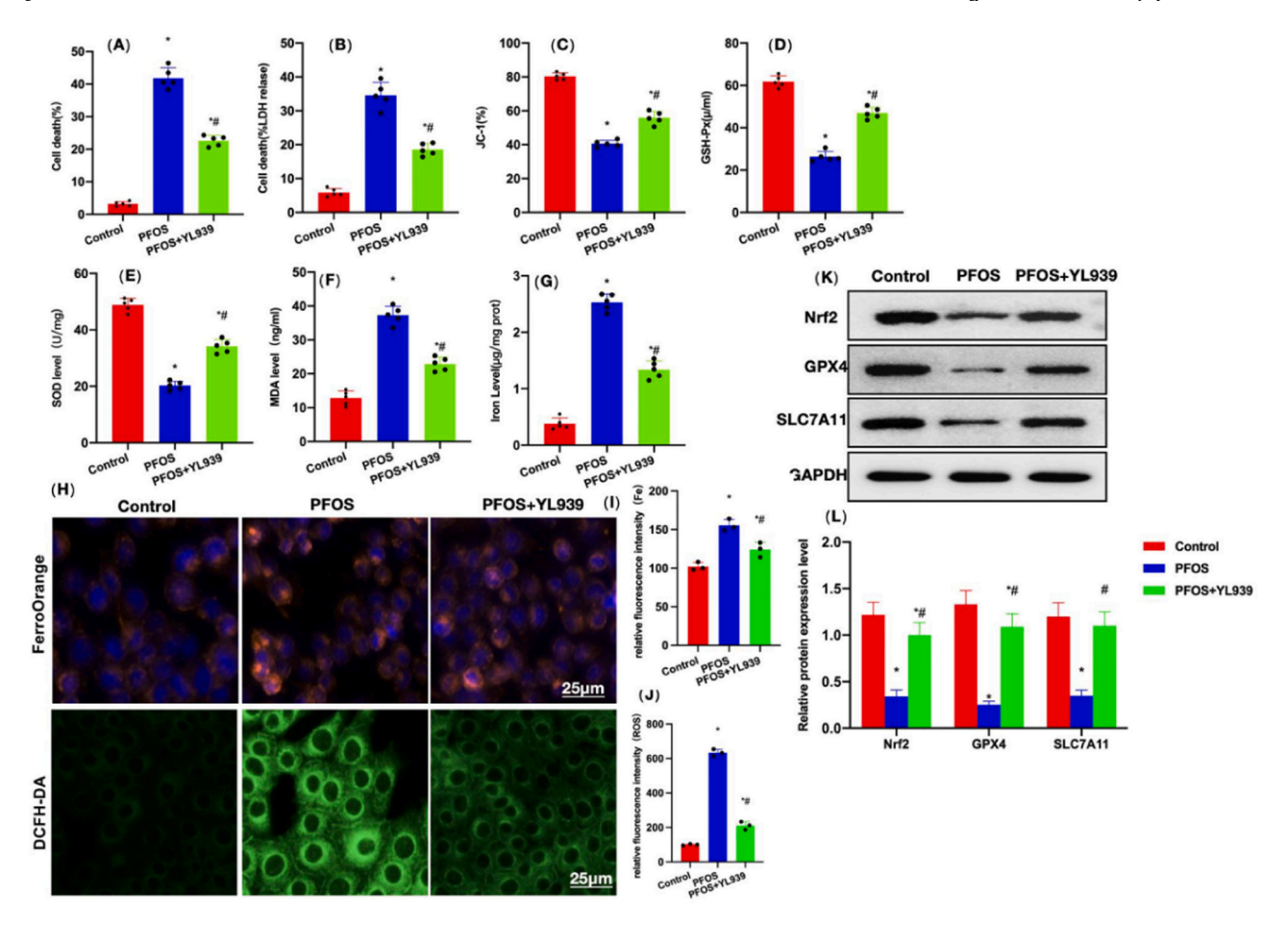


Fig. 2. : ROS inhibitor could inhibit PFOS-induced hepatocyte ferroptosis. A-B: Cytotoxicity (n = 5), the PFOS+BABTA group exhibited lower cell mortality and LDH release rates compared to the PFOS group C: JC-1 (n = 5), the proportion of JC-1 was higher in the PFOS+BABTA group than in the PFOS group D-F: GSH-Px, MDA and SOD (n = 5), in relative to the PFOS group, the levels of GSH-Px and SOD were higher, while the level of MDA was lower in the PFOS-BABTA group G: Iron ion (n = 5), the  $Fe^{2+}$  level was lower in the PFOS+BABTA group than in the PFOS group H-J: IF (n = 5), BABTA could inhibit the ROS level and reduce the fluorescence intensity, while in  $Fe^{2+}$  staining, BABTA did not affect the fluorescence intensity, showing insignificant difference from the PFOS group K-L: The Nrf2, GPX4 and SLC7A11 levels were higher in the PFOS+BABTA group than in the PFOS group. \*P < 0.05 vs. Control;  $^{\#}P < 0.05$  vs. PFOS.

For the Fe $^{2+}$  staining with FerroOrange probe, 35  $\mu l$  of DMSO was added into FerroOrange (24  $\mu g)$  to prepare 1 mM FerroOrange stock solution. The prepared stock solution was diluted with neutral buffer or cell medium to the required working concentration of 1  $\mu M$ . After 24 h of treatment with PFOS and washing with PBS, the hepatocytes were stained using FerroOrange probe solution, and excited using a 532-nm laser with an emission wavelength of 572 nm. Fe $^{2+}$  staining produced orange fluorescence.

#### 2.6. GSH-Px, MDA and SOD assays

Detection was accomplished with GSH-Px, MDA and SOD kits (Jiancheng Bioengineering Institute, Nanjing, China). After homogenizing mouse liver tissues, the hepatocyte membranes were broken and centrifuged at 2500 g. Thereafter, the supernatant was collected, supplemented with reagents in line with the kit instructions, and subject to incubation at 37  $^{\circ}\text{C}$  for 20 min, followed by detection of OD values at 450 nm.

#### 2.7. ROS assay

DCDH-DA probe (SIGMA, MA, USA) was utilized for detecting ROS levels. The cells were inoculated into 6-well microplates, subject to treatment with PFOS for 24 h and then washed with PBS. Each well was supplemented with 1 mL (  $10~\mu M$  ) of DCFH-DA probe-containing

medium, and the incubation continued for 30 min in an incubator. The medium was discarded and the cells were rinsed twice with serum-free medium. Fluorescent microscope was used to observe the staining level of cells and fluorescent spectrophotometer was applied to measure the absorbance.

#### 2.8. Animal model

SPF C57BL/6 mice were purchased from Cyagen Biosciences, which were classified into 10 mice per group. In addition, a mouse model of liver injury was established by intraperitoneally injecting PFOS at 500  $\mu$ g/kg once daily for 7 consecutive d. Meanwhile, we also administered the ferroptosis inhibitor YL939 and ROS inhibitor BABTA together with PFOS once daily. Later, the mice were killed 7 d for assays.

# 2.9. H&E

After paraffin embedding, mouse liver tissue was sectioned in consecutive 4 m sections. Later, the sections were processed by xylene deparaffinization, gradient alcohol dehydration, hematoxylin staining for 3 mins, washing with running water for 2 mins, and treatment with 1% saline alcohol for another 2 s. Sections were then rinsed with running water for 2 mins, followed by 1% ammonia treatment for 20 s, 0.5% eosin alcohol staining for 10 s, gradient alcohol dehydration, xylene permeabilization, and neutral Gum sealant. An optical microscope was

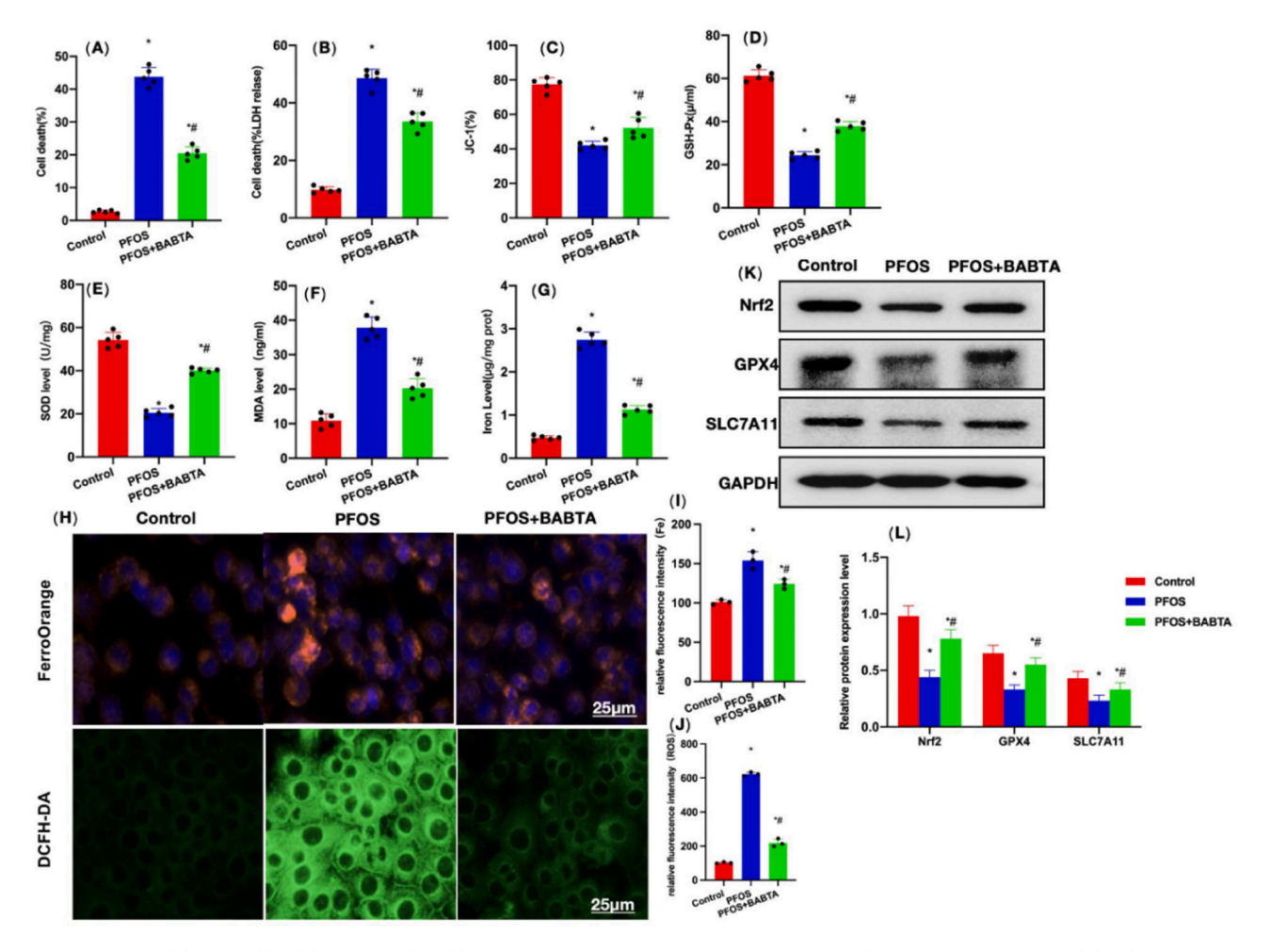


Fig. 3. : Ferroptosis inhibitor could inhibit PFOS-induced hepatocyte ferroptosis. A-B: Cytotoxicity (n = 5), the PFOS+YL939 group exhibited lower rates of cell mortality and LDH release than the PFOS group C: JC-1 (n = 5), the proportion of JC-1 was higher in the PFOS+YL939 group than in the PFOS group D-F: GSH-Px, MDA and SOD (n = 5), the PFOS-YL939 group exhibited higher GSH-Px and SOD levels, while lower MDA level compared to the PFOS group G: Iron ion (n = 5), the Fe<sup>2+</sup> level was lower in the PFOS+YL939 group than in the PFOS group H-J: IF (n = 5), YL939 could inhibit the level of ferroptosis and weaken the Fe<sup>2+</sup> fluorescence intensity, which though did not affect the ROS fluorescence intensity in ROS staining K-L: The Nrf2, GPX4 and SLC7A11 levels were higher in the PFOS+YL939 group than in the PFOS group. \*P < 0.05 vs. Control;  $^{\#}P$  < 0.05 vs. PFOS.

used to observe the histopathological changes of the liver.

# 2.10. Oil red O staining

The staining solution was prepared in the oil red-O staining kit (Shanghai YEASEN Biotechnology Co., Ltd, Shanghai, China) in a stock solution:diluent ratio of 5:2. Later, the sections were placed in the staining solution for 15 mins, rinsed in 37% distilled water for 15 s, counterstained for 5 mins, and washed with water for 45 s. After assembly, the sections were viewed under the microscope.

# 2.11. AST and ALT assays

After 7 d of continuous PFOS administration, mouse tail venous bloods were sampled, centrifuged and then the supernatant was gathered. ALT and AST were detected by ultraviolet colorimetry (Jiancheng Bioengineering Institute, Nanjing, China) in accordance with the kit instructions. The obtained results were shown as U/L.

#### 2.12. Western-blotting

After homogenization of tissues, the tissue homogenate and cells were lysed on ice with NP-40 buffer for 30 min, and later exposed to BCA  $\,$ 

protein quantification. Electrophoresis separation was performed with 8–12% SDS-PAGE gel at 80–120 V voltage, and the membranes were transferred at a 300-mA constant flow, followed by 2 h of blockade with 5% skim milk powder. Thereafter, the membranes were incubated with TBST-diluted primary monoclonal antibody (Abcam, MA, USA), and further with HRP-labeled goat anti-rabbit secondary antibody (Abcam, USA). The membranes were identified by chemiluminescent immuno-assay. The OD was analyzed through Image Pro-Plus 6.0.

#### 2.13. Statistical methods

All the measurement data were shown as (Mean  $\pm$  SE), and processed via SPSS 17.0. Following homogeneity of variance test, two groups of data were explored through two independent samples t-test, while three or more groups of data were studied through one-way ANOVA. LSD method was used to make all the subsequent inter-group pairwise comparisons. All of the above test processes were two-sided. The differences were thought to be of statistical significance when P <0.05.

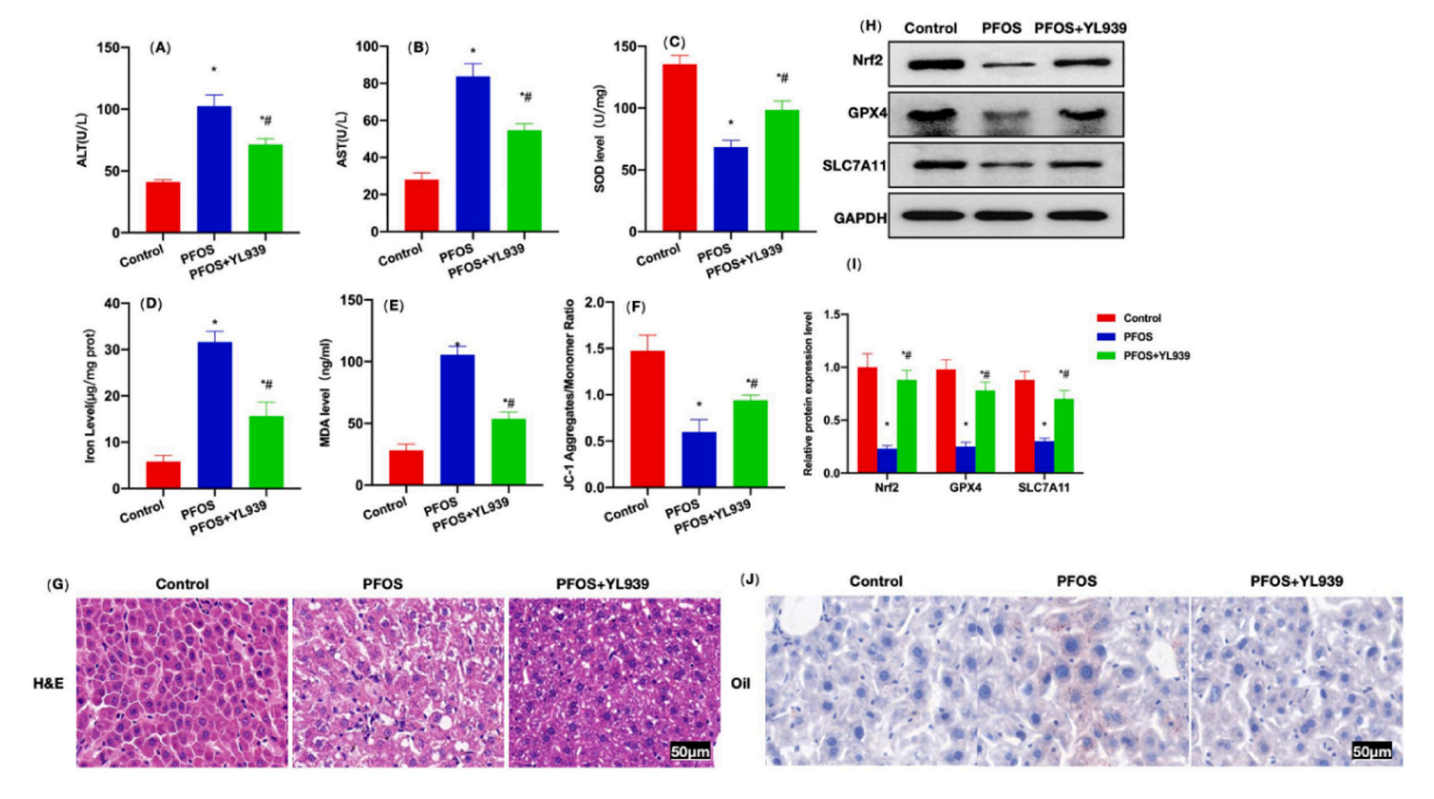


**Fig. 4.** : PFOS induced liver injury through ferroptosis. A-B: ALT and AST (n=10), PFOS could elevate the levels of ALT and AST, while YL939 could inhibit such levels, exhibiting obvious differences from the PFOS group C-F: PFOS could elevate the tissue  $Fe^{2+}$  level, increase the MDA level, lower the JC1 proportion, and reduce the SOD expression. Meanwhile, YL939 could elevate the SOD level, lower the levels of  $Fe^{2+}$  and MDA, and increase the JC1 proportion, exhibiting significant differences from the PFOS group G: H&E (n=5), evident tissue inflammation and edema were noted in the PFOS group, while in the YL939 group, the inflammation of liver tissues was weakened I: Relative protein expressions (n=5), higher levels of Nrf2, GPX4 and SLC7A11 were noted in the PFOS+YL939 group than in the PFOS group J:Oil O Red (n=5): lipid deposition in PFOS, which is significantly different from Control. YL939 can inhibit lipid deposition. \*P < 0.05 vs. Control; \*P < 0.05 vs. PFOS.

#### 3. Results

#### 3.1. PFOS induced ferroptosis of hepatocytes

The LD50 of PFOS was 55 M in 24 h [Fig. 1A]. The cytotoxicity test revealed that PFOS could trigger the hepatocyte injury and increase the intracellular LDH level [Fig. 1B-C]. The JC-1 results showed mitochondrial damage in the PFOS group and significantly reduced JC-1 content [Fig. 1D]. Consistent with the test results of oxidative stress indices, PFOS could downregulate GSH-Px and SOD levels and increase MDA levels [Fig. 1E-G]. An iron ion test revealed that PFOS can increase intracellular iron ion levels [Fig. 1H]. Fluorescence staining showed that iron ion and ROS levels were significantly increased in the PFOS group and the fluorescence intensity was higher than that in the control group [Fig. 1I-K]. Protein assays revealed that PFOS can suppress the levels of Nrf2, GPX4 and SLC7A11, trigger oxidative damage and promote the occurrence of ferroptosis [Fig. 1L-M].

#### 3.2. ROS inhibitor could inhibit PFOS-induced hepatocyte ferroptosis

Inhibition of ROS by BABTA could antagonize the PFOS-induced ferroptosis in hepatocytes. Cytotoxicity test revealed that the rates of cell mortality and LDH release in the PFOS+BABTA group were lower than those in the PFOS group [Fig. 2A-B]. The proportion of JC-1 was higher in the PFOS+BABTA group than in the PFOS group [Fig. 2C]. Based on the results of oxidative stress indices, the PFOS-BABTA group showed higher levels of GSH-Px and SOD, as well as lower level of MDA compared to the PFOS group [Fig. 2D-F]. Iron ion assay demonstrated that the Fe<sup>2+</sup> level was lower in the PFOS+ BABTA group than in the PFOS group [Fig. 2G]. IF staining demonstrated that BABTA could

inhibit ROS levels and weaken fluorescence intensity, while in  ${\rm Fe}^{2+}$  staining, BABTA did not affect fluorescence intensity, showing insignificant difference from the PFOS group [Fig. 2H-J]. As suggested by the detection of relative protein expressions, the levels of Nrf2, GPX4 and SLC7A11 were higher in the PFOS+BABTA group than in the PFOS group [Fig. 2K-L].

# 3.3. Ferroptosis inhibitor could inhibit PFOS-induced hepatocyte ferroptosis

Treatment with YL939 could antagonize the PFOS-induced ferroptosis in hepatocytes. Cytotoxicity test demonstrated that the cell mortality and LDH release rates were lower in the PFOS+YL939 group than in the PFOS group [Fig. 3A-B]. PFOS+YL939 group exhibited higher proportion of JC-1 compared to the PFOS group [Fig. 3C]. In line with the results of oxidative stress indices, the PFOS-YL939 group exhibited higher levels of GSH-Px and SOD, while lower level of MDA compared to the PFOS group [Fig. 3D-F]. As revealed by the iron ion assay, the Fe<sup>2+</sup> level in the PFOS+YL939 group was lower than that in the PFOS group [Fig. 3G]. IF staining demonstrated that YL939 could inhibit the ferroptosis level and weaken the Fe<sup>2+</sup> fluorescence intensity, while in ROS staining, YL939 did not affect the fluorescence intensity of ROS, showing insignificant difference from the PFOS group [Fig. 3H-J]. Detection of relative protein expressions found that the levels of Nrf2, GPX4 and SLC7A11 were higher in the PFOS+YL939 group than in the PFOS group [Fig. 3K-L].

# 3.4. PFOS induced liver injury through ferroptosis

We injected PFOS intraperitoneally, finding that its accumulation

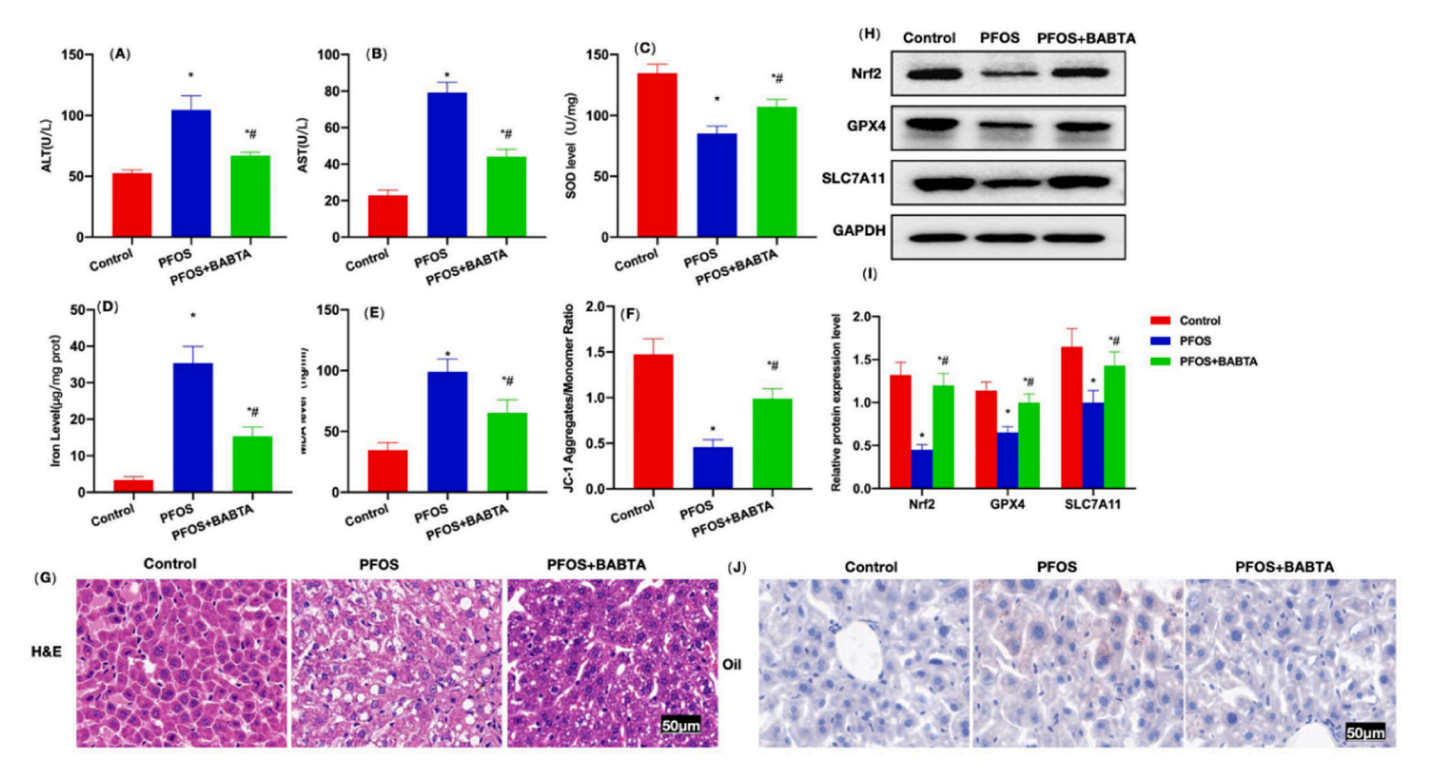


Fig. 5. : ROS inhibitor could inhibit PFOS-induced liver injury. A-B: ALT and AST (n=10), BABTA could inhibit the ALT and AST levels, exhibiting obvious differences from the PFOS group C-F: BABTA could elevate the SOD level, lower the levels of Fe<sup>2+</sup> and MDA, and increase the JC1 proportion, exhibiting obvious differences from the PFOS group G: H&E (n=5), evident tissue inflammation and edema were noted in the PFOS group, while in the BABTA group, the inflammatory response of liver tissues was weakened H-I: Relative protein expressions (n=5), the levels of Nrf2, GPX4 and SLC7A11 were higher in the PFOS+BABTA group than in the PFOS group J:Oil O Red (n=5): lipid deposition in PFOS, which is significantly different from Control. BABTA can inhibit lipid deposition. \*P < 0.05 vs. Control; \*P < 0.05 vs. PFOS.

could induce liver injury, while treatment with YL939 could inhibit liver injury. Detection of liver function discovered that PFOS could elevate the levels of ALT and AST, while YL939 could inhibit such levels, revealing significant differences from the PFOS group [Fig. 4A-B]. PFOS could increase the tissue Fe<sup>2+</sup> level, increase the MDA level, lower the JC1 proportion, and reduce the SOD expression. Meanwhile, YL939 could elevate the SOD level, lower the levels of Fe2+ and MDA, and increase the JC1 proportion, showing significant differences from the PFOS group [Fig. 4C-F]. H&E staining revealed evident tissue inflammation and edema in the PFOS group, while in the YL939 group, the inflammation of liver tissues was weakened [Fig. 4G]. Detection of relative protein expressions revealed that the levels of Nrf2, GPX4 and SLC7A11 were higher in the PFOS+YL939 group than in the PFOS group [Fig. 4H-I]. Oil Red O staining shows lipid deposition in PFOS, which is significantly different from Control. YL939 can inhibit lipid deposition. [Fig. 4J].

#### 3.5. ROS inhibitor could inhibit PFOS-induced liver injury

Treatment with BABTA could inhibit the liver injury. Detection of liver function discovered that PFOS could elevate the levels of ALT and AST, while BABTA could suppress such levels, exhibiting obvious differences from the PFOS group [Fig. 5A-B]. PFOS could elevate the tissue Fe<sup>2+</sup> level, increase the MDA expression, lower the JC1 proportion, and reduce the SOD expression. Meanwhile, BABTA could elevate the SOD level, lower the levels of Fe<sup>2+</sup> and MDA, and increase the JC1 proportion, showing significant differences from the PFOS group [Fig. 5C-F]. H&E staining revealed evident tissue inflammation and edema in the PFOS group, while in the BABTA group, the inflammatory response of liver tissues was weakened [Fig. 5G]. As revealed by the assays of relative protein expressions, the levels of Nrf2, GPX4 and SLC7A11 were higher in the PFOS+BABTA group than in the PFOS group [Fig. 5H-I].

Oil Red O staining shows lipid deposition in PFOS, which is significantly different from Control. BABTA can inhibit lipid deposition [Fig. 5J].

#### 4. Discussion

Unlike other forms of cell death such as pyroptosis, autophagy and apoptosis (Miyauchi et al., 2023), ferroptosis is iron dependent and also associated with extensive lipid peroxidation (Liu et al., 2022). As shown in many articles, ferroptosis has a crucial impact on the pathogenic mechanism of various liver diseases (Shi et al., 2023), such as: B. Hepatitis C virus (HCV) infection, alcoholic liver disease (ALD), hemochromatosis (Huang et al., 2023) and non-alcoholic steatohepatitis (NASH) as well as hepatocellular carcinoma (HCC) (Gao et al., 2023a). Free iron is involved in the production of reactive oxygen species (ROS) through the Fenton reaction, whereby the accumulation of ROS leads to oxidative cell death, which is the essence of ferroptosis (Sun et al., 2023). Currently, oxidative stress injury (Nrf2 signaling regulation) and lipid metabolism damage play a crucial role in the regulation of ferroptosis (Gao et al., 2023b). Ferroptosis has a major impact on acute liver injury (ALI), a disease characterized by a rapid decline in the patient's hepatocyte function (Qiu et al., 2023). In most cases, ALI is caused by drugs, alcohol, ischemia/reperfusion injury (IRI), or viral hepatitis (He and Shi, 2023). However, the ferroptosis inhibitor Liproxstatin-1 (Lip-1) can significantly reduce liver and kidney IRI (Kar et al., 2023), suggesting an important pathogenic role of ferroptosis in ALI.A recent study involving human volunteers found that elevated serum ferritin levels in liver donors are associated with a significantly increased risk of liver injury in transplant recipients and that the use of Fer-1 and -tocopherol can block ferroptosis to prevent ALI (Huo et al., 2023). GPX4, as a key to cell survival and a central regulatory protein of ferroptosis, can inhibit lipid peroxidation by degrading small molecule peroxides and some lipid peroxides (Li et al., 2023b). If phospholipid

hydroperoxides are not effectively quenched by GPX4, they can trigger catalytic reactions in the presence of transition metals (e.g. iron), ultimately leading to cell death (Wei et al., 2023). Meanwhile, downregulation of GPX4 in cells is more sensitive to ferroptosis, and knocking down GPX4 can trigger ferroptosis. On the contrary, when GPX4 expression is upregulated, tolerance to ferroptosis can be developed (Zhai et al., 2023; Ding et al., 2023).

After biological ingestion, PFOS is generally not stored in adipose tissues, most of which binds to plasma proteins to exist in the blood, while the rest partly accumulates in the liver and muscle tissues of animals. Thus, prolonged PFOS exposure and intrahepatic accumulation can induce liver injury. Overall, our results found that PFOS induced hepatocyte ferroptosis through ROS, thereby leading to liver injury. PFOS can cause hepatocyte damage in vitro. A combination of LDH, a cytotoxicity quantifying technique, with CCK-8 assay found that PFOS could induce hepatocyte damage. In the meantime, oxidative stress injury was activated, the levels of GSH-Px and SOD were downregulated, while the level of MDA was upregulated. Noteworthy is that PFOS increased the levels of Fe2 + and ROS, and that Fenton reaction involving Fe2 + and ROS is the basic event of ferroptosis. Hence, we consider that PFOS induces hepatocyte injury through ferroptosis. Meanwhile, the levels of GPX4, SLC7A11 and Nrf2 were also downregulated. Nrf2 is an important regulatory signal for oxidative stress and ferroptosis, while GPX4 and SLC7A11 are the core proteins that regulate lipid oxidation and ferroptosis. Decreased levels of these three indicate that PFOS activates ferroptosis via oxidative stress damage. We also treated cells with ferroptosis and ROS inhibitors and found that they can inhibit ferroptosis and cell damage and increase the levels of Nrf2, GPX4 and SLC7A11. Through in vitro experiments, we demonstrated that PFOS activates ROS-mediated ferroptosis and causes liver damage. As the results of animal studies also show, the ferroptosis and ROS inhibitors can alleviate PFOS-induced liver injury, improve the liver function of mice, reduce ALT and AST levels, improve oxidative stress damage, and at the same time inhibit the level of fibrosis Liver damage and an increase in GPX4 levels.

#### 5. Conclusion

Our study shows that PFOS can trigger hepatocyte injury through ROS-mediated ferroptosis, thereby causing liver injury. Ferroptosis is one of the main mechanisms for PFOS-mediated liver damage. The use of ferroptosis and ROS inhibitors can inhibit PFOS-induced liver injury. Furthermore, the results of the current work provide a novel reference for the environmental toxicology and treatment of PFOS.

#### Ethical approval and consent to participate

The study approval with Ethics Committee.

# **Funding**

Zhejiang Medical and Health Plan Project [2021KY353], [2021KY1112].

# CRediT authorship contribution statement

Yang Yang, Liuwei Xie and Yu Zhu: Experimental operation and data acquisition. Yongjia Sheng, Jin Wang, Xiaohong Zhou: Experiment Design and Data Statistical Analysis. Wenyan Li: Project fund support. i Chenxi Cao, Yi Yang. Chenyang Han: Article writing and revision.

# **Declaration of Competing Interest**

We have no conflicts of interest to declare.

#### **Data Availability**

The authors are unable or have chosen not to specify which data has been used.

#### Acknowledgement

I need to thank my colleagues and friends for their help and support in the research , Thanks for the support of Funding.

# Consent for publication

All authors approval published the article.

#### References

- Ding, J., Lu, B., Liu, L., Zhong, Z., Wang, N., Li, B., Sheng, W., He, Q., 2023. Guilu-Erxian-Glue alleviates Tripterygium wilfordii polyglycoside-induced oligoasthenospermia in rats by resisting ferroptosis via the Keap1/Nrf2/GPX4 signaling pathway. Pharm. Biol. 61 (1), 213–227.
- Gao, G., Zhou, J., Wang, H., Ke, L., Zhou, J., Ding, Y., Ding, W., Zhang, S., Rao, P., 2023a. Fish oil nano-emulsion kills macrophage: ferroptosis triggered by catalase-catalysed superoxide eruption. Food Chem. 408, 135249.
- Gao, J., Wang, Q., Tang, Y.D., Zhai, J., Hu, W., Zheng, C., 2023b. When ferroptosis meets pathogenic infections. Trends Microbiol. 31 (5), 468–479.
- He, L., Shi, Y., 2023. Reduced glutathione ameliorates acute kidney injury by inhibiting ferroptosis. Mol. Med. Rep. 27 (6), 123.
- Huang, J., Xie, H., Yang, Y., Chen, L., Lin, T., Wang, B., Lin, Q.C., 2023. The role of ferroptosis and endoplasmic reticulum stress in intermittent hypoxia-induced myocardial injury. Sleep. Breath. 27 (3), 1005–1011.
- Huo, L., Liu, C., Yuan, Y., Liu, X., Cao, Q., 2023. Pharmacological inhibition of ferroptosis as a therapeutic target for sepsis-associated organ damage. Eur. J. Med. Chem. 257, 115438.
- Kar, F., Yıldız, F., Hacioglu, C., Kar, E., Donmez, D.B., Senturk, H., Kanbak, G., 2023. LoxBlock-1 or Curcumin attenuates liver, pancreas and cardiac ferroptosis, oxidative stress and injury in Ischemia/reperfusion-damaged rats by facilitating ACSL/GPx4 signaling. Tissue Cell 82, 102114.
- Li, P., Yu, J., Huang, F., Zhu, Y.Y., Chen, D.D., Zhang, Z.X., Xie, Z.C., Liu, Z.Y., Hou, Q., Xie, N., Peng, T.H., Chen, X., Li, L., Xie, W., 2023b. SLC7A11-associated ferroptosis in acute injury diseases: mechanisms and strategies. Eur. Rev. Med. Pharm. Sci. 27 (10), 4386–4398.
- Li, S., Wen, P., Zhang, D., Li, D., Gao, Q., Liu, H., Di, Y., 2023a. PGAM5 expression levels in heart failure and protection ROS-induced oxidative stress and ferroptosis by Keap1/Nrf2. Clin. Exp. Hypertens. 45 (1), 2162537.
- Liu, C., Zou, Q., Tang, H., Liu, J., Zhang, S., Fan, C., Zhang, J., Liu, R., Liu, Y., Liu, R., Zhao, Y., Wu, Q., Qi, Z., Shen, Y., 2022. Melanin nanoparticles alleviate sepsis-induced myocardial injury by suppressing ferroptosis and inflammation. Bioact. Mater. 24, 313–321.
- Liu, C., Shen, Y., Cavdar, O., Huang, J., Fang, H., 2023b. Angiotensin II-induced vascular endothelial cells ferroptosis via P53-ALOX12 signal axis. Clin. Exp. Hypertens. 45 (1), 2180019.
- Liu, Y., Yu, G., Zhang, R., Feng, L., Zhang, J., 2023a. Early life exposure to low-dose perfluorooctane sulfonate disturbs gut barrier homeostasis and increases the risk of intestinal inflammation in offspring. Environ. Pollut. 329, 121708.
- Miyauchi, W., Shishido, Y., Matsumi, Y., Matsunaga, T., Makinoya, M., Shimizu, S., Miyatani, K., Sakamoto, T., Umekita, Y., Hasegawa, T., Fujiwara, Y., 2023. Simultaneous regulation of ferroptosis suppressor protein 1 and glutathione peroxidase 4 as a new therapeutic strategy of ferroptosis for esophageal squamous cell carcinoma. Esophagus 20 (3), 492–501.
- Mohona, T.M., Ye, Z., Dai, N., Nalam, P.C., 2023. Adsorption behavior of long-chain perfluoroalkyl substances on hydrophobic surface: A combined molecular characterization and simulation study. Water Res 239, 120074.
- Phelps, D.W., Palekar, A.I., Conley, H.E., Ferrero, G., Driggers, J.H., Linder, K.E., Kullman, S.W., Reif, D.M., Sheats, M.K., DeWitt, J.C., Yoder, J.A., 2023. Legacy and emerging per- and polyfluoroalkyl substances suppress the neutrophil respiratory burst. J. Immunotoxicol. 20 (1), 2176953.
- Qian, Y., Chen, L., Gao, B., Ye, X., 2023. Sestrin2 levels in patients with anxiety and depression myocardial infarction was up-regulated and suppressed inflammation and ferroptosis by LKB1-mediated AMPK activation. Clin. Exp. Hypertens. 45 (1), 2205049
- Qiu, S., Li, X., Zhang, J., Shi, P., Cao, Y., Zhuang, Y., Tong, L., 2023. Neutrophil membrane-coated taurine nanoparticles protect against hepatic ischemiareperfusion injury. Eur. J. Pharm. 949, 175712.
- Rudzanova, B., Vlaanderen, J., Kalina, J., Piler, P., Zvonar, M., Klanova, J., Blaha, L., Adamovsky, O., 2023. Impact of PFAS exposure on prevalence of immune-mediated diseases in adults in the Czech Republic. Environ. Res 229, 115969.
- Shi, X., Feng, D., Han, P., Wei, W., 2023. Ferroptosis-related ACSL3 and ACTC1 predict metastasis-free survival for prostate cancer patients undergoing radical radiotherapy. Asian J. Surg. 46 (6), 2489–2490.

- Sun, X., Zhang, X., Yan, H., Wu, H., Cao, S., Zhao, W., Dong, T., Zhou, A., 2023. Protective effect of curcumin on hepatolenticular degeneration through copper excretion and inhibition of ferroptosis. Phytomedicine 113, 154539.
- Wang, Z., Zang, L., Ren, W., Guo, H., Sheng, N., Zhou, X., Guo, Y., Dai, J., 2023. Bile acid metabolism disorder mediates hepatotoxicity of Nafion by-product 2 and perfluorooctane sulfonate in male PPARα-KO mice. Sci. Total Environ. 876, 162579.
- Wei, Y., Gao, C., Wang, H., Zhang, Y., Gu, J., Zhang, X., Gong, X., Hao, Z., 2023. Mori fructus aqueous extracts attenuates liver injury by inhibiting ferroptosis via the Nrf2 pathway. J. Anim. Sci. Biotechnol. 14 (1), 56.
- Wu, S., Yuan, T., Fu, W., Dong, H., Zhang, Y., Zhang, M., Jiang, C., Xu, Q., Zhang, L., Qiang, Z., 2023. Perfluorinated compound correlation between human serum and drinking water: is drinking water a significant contributor? Sci. Total Environ. 873, 162471.
- Zhai, H., Zhong, S., Wu, R., Mo, Z., Zheng, S., Xue, J., Meng, H., Liu, M., Chen, X., Zhang, G., Zheng, X., Du, F., Li, R., Zhou, B., 2023. Suppressing circIDE/miR-19b-3p/RBMS1 axis exhibits promoting-tumour activity through upregulating GPX4 to diminish ferroptosis in hepatocellular carcinoma. Epigenetics 18 (1), 2192438.
- Zhang, L., Zheng, X., Liu, X., Li, J., Li, Y., Wang, Z., Zheng, N., Wang, X., Fan, Z., 2023. Toxic effects of three perfluorinated or polyfluorinated compounds (PFCs) on two strains of freshwater algae: Implications for ecological risk assessments. J. Environ. Sci. (China) 131, 48–58.
- Zhao, N., Jin, H., Mao, W., Zhao, M., Chen, Y., 2023. Concentrations and isomer profiles of perfluoroalkyl carboxylates in house rats (Rattus norvegicus) and human blood: Implication for human exposure sources. Sci. Total Environ. 881, 163431.